

# Optimal packing of polydisperse hard-sphere fluids II

Ronald Blaak

*University of Amsterdam, Faculty for Mathematics, Computer Science, Physics and Astronomy,  
Kruislaan 403, 1098 SJ Amsterdam, The Netherlands*

(February 1, 2008)

## Abstract

We consider the consequences of keeping the total surface fixed for a polydisperse system of  $N$  hard spheres. In contrast with a similar model (J. Zhang *et al.*, J. Chem. Phys. **110**, 5318 (1999)), the Percus-Yevick and Mansoori equations of state work very well and do not show a breakdown. For high pressures Monte Carlo simulation we show three mechanically stable polydisperse crystals with either a unimodal or bimodal particle-size distributions.

## I. INTRODUCTION

Colloidal suspensions are never truly monodisperse, but are in general polydisperse. This might lead to unfavorable behavior, because it will for example not be possible to form a high quality crystal. Polydispersity will also have consequences on other properties like the viscosity of the system. A better understanding of these systems could therefore possibly lead to a handle to tune some of the relevant properties of colloidal suspensions.

In a recent paper<sup>1</sup> we considered a system of  $N$  hard spheres of which the total volume is fixed. The spheres are, however, allowed to exchange volume under this constraint. Theory and Monte Carlo simulations showed that the Percus-Yevick (PY) theory, which normally is well suited for describing a polydisperse hard sphere system, has a breakdown at a low volume fraction ( $\eta \approx 0.260$ ). According to the theoretical description, the size-distribution function of the particles can not be normalized above this threshold. In simulations it is found that above this packing fraction a few of the particles will grow bigger on increasing pressure. They will contain most of the available volume and will be surrounded by a sea of small particles. The size of these big particles becomes of the order of the simulation box, therefore finite size effects do not allow to conclude how to describe the system at high pressures.

In this article we will focus on a similar system, but now the total surface of the particles is fixed. In the Monte Carlo simulations we performed, we allowed particles to exchange amounts of surface under the constraint that the total surface remains constant. An experimental system with this type of behavior, would be a system of surfactant molecules, which are free to aggregate into spherical micelles. For this model system we derive the Helmholtz free energy, which is given by the free energy of a polydisperse system with an arbitrary size-distribution, subject to two constraints, both the number of particles and the

total surface of the particles are fixed. We define the optimal size-distribution of this system as the one that minimizes this restricted Helmholtz free energy.

The remainder of this paper is organized as follows: in Sec. II we derive the Helmholtz free energy of this system and calculate the optimal size-distribution. In Sec. III we show the results of our computer simulations and make a comparison with the theoretical predictions. In Sec. IV we discuss the possibilities to form a high density crystalline phases and conclude in Sec. V with a discussion of our results.

## II. THEORY

In a multicomponent system the ideal entropy is given by a simple expression

$$-Nk_B \sum_i w_i \ln(\Lambda_i^3 \rho w_i), \quad (1)$$

where  $w_i$  is the molar fraction of species  $i$  and  $\Lambda_i$  its thermal wavelength. In a true polydisperse system, however, this entropy is infinite<sup>2</sup>. Normally one would describe such a system by distributing the particles over boxes according to some property, e.g. diameter or volume, which would enable us to distinguish them. In the case of a fixed particle-size distribution this is perfectly allowed for whatever property one wishes to choose. In our case, however, the particle-size distribution is allowed to change and as a consequence the labeling property will influence the theoretical description of the system<sup>1</sup>. The choice of how to label the different boxes is in fact determined by an a priori probability assumption, which in this case is dictated by the way polydispersity is sampled.

The way we sample the polydispersity can be thought of to describe a system with a large, constant number of tiny particles, which form  $N$  spherical aggregates. Exchanging surface between the aggregates would then imply exchanging some of these tiny particles. The number of these particles forming the aggregate is proportional to the surface, which forms a natural labeling of our system.

The fact that the total surface of the  $N$  spherical particles is conserved leads to a natural length scale  $\langle \sigma^2 \rangle^{(1/2)}$ , where  $\sigma$  is the diameter of a particles and  $\langle \cdot \rangle$  denotes an average over particle-size distributions. We introduce the reduced pressure  $P^* = (k_B T)^{-1} P \langle \sigma^2 \rangle^{(3/2)}$ , where  $k_B T$ , the Boltzmann constant times the temperature  $T$ , is our unit of energy.

For an  $n$ -component hard sphere mixture, the compressibility pressure in the Percus-Yevick approximation yields<sup>2</sup>:

$$\frac{\pi}{6} P^* = \frac{\xi_0}{1 - \xi_3} + \frac{3\xi_1 \xi_2}{(1 - \xi_3)^2} + \frac{3\xi_2^3}{(1 - \xi_3)^3}, \quad (2)$$

where the  $j$ -moment of the particle-size distribution  $\xi_j$  is defined as

$$\xi_j = \frac{\pi}{6} \sum_i \rho_i \sigma_i^j, \quad (3)$$

where the index  $i$  is used to denote the different particle species,  $\rho_i = N_i/V$  is their number density, and  $\sigma_i$  is their diameter.

Equation (2) is also valid for a continuous size-distribution, in which case the sum in Eq. (3) is replaced by an integral. The corresponding expression for the chemical potential of a species with diameter  $\sigma$  is<sup>3</sup>

$$\mu^* = \ln [\rho \Lambda^3 W(s)] - \ln(1 - \xi_3) + \frac{3\xi_2\sigma}{(1 - \xi_3)} + \frac{3\xi_1\sigma^2}{(1 - \xi_3)} + \frac{9\xi_2^2\sigma^2}{2(1 - \xi_3)^2} + \frac{\pi}{6} P^* \sigma^3, \quad (4)$$

where  $\Lambda$  is the de-Broglie thermal wavelength,  $\sqrt{\hbar^2/(2\pi mkT)}$ , and  $W(s)$  is the probability density to find a particle with a surface around  $s = \pi\sigma^2$ . The pressure  $P^*$  is given by Eq. (2).

In an (NPT) description, the Gibbs free energy  $\mathcal{G}$  of the system fulfilling the constraints, must be at a minimum, and is given by the following functional

$$\mathcal{G}[W(s)] = \int \mu^* W(s) ds - \mathcal{L}_0 \int W(s) ds - \mathcal{L}_1 \int s W(s) ds. \quad (5)$$

The Lagrange multipliers  $\mathcal{L}_0$  and  $\mathcal{L}_1$  ensure that the conservation of the number of particles and of the total amount of surface respectively are satisfied. For a minimum of the Gibbs free energy the functional derivative of  $\mathcal{G}$  with respect to  $W(s)$  should be zero, which implies that  $W(s)$  must be of the form:

$$W(s) = \exp \left\{ \sum_{i=0}^3 \alpha_i \sigma^i \right\}, \quad (6)$$

where the values of  $\alpha_1$  and  $\alpha_3$  are explicitly given by

$$\alpha_1 = -\frac{3\xi_2}{1 - \xi_3}, \quad (7)$$

$$\alpha_3 = -\frac{\pi}{6} P^*. \quad (8)$$

The coefficients  $\alpha_0$  and  $\alpha_2$  are determined by the constraints on the number of particles and the total of available surface. Note that all  $\xi_i$  ( $i = 1, 2, 3$ ) are positive. Moreover,  $\xi_3$  is equal to the volume fraction  $\eta$ , and is therefore necessarily less than one. Hence,  $\alpha_1$  and  $\alpha_3$  are always negative. This also implies that the particle-size distribution can always be normalized. This is different from our previous model<sup>1</sup>, where the constraint on the total volume implied that  $\alpha_3$  could be zero and gave rise to a critical endpoint on the equation of state, beyond which the PY-theory is not capable of describing that system. In this case, however, it is  $\alpha_2$  which can change sign and become positive due to the constraint on the surface. This will lead to the formation of bimodal particle-size distributions in this model. An argument similar to the one used in Ref.<sup>1</sup> to show the break down of the Percus-Yevick equation of state, can also be used here to show that no break down will occur in this case, where the total surface of the particles is constrained<sup>4</sup>.

By self-consistently solving Eqns. (7), (8) and the two equations imposed by the constraints, we obtain the equation of state of this model (Figs. 1 and 2) and the particle-size distributions in equilibrium according to the PY-theory. The equation of state is presented here both as function of the packing fraction  $\eta$  and reduced density  $\rho^* = (N/V)\langle\sigma^2\rangle^{(3/2)}$ ,

because in contrast with most simulations the volume of the particles involved is not constant.

In the limit where the density goes to zero  $\alpha_1 = \alpha_3 = 0$  and the particle-size distribution function  $W(s)$  is an exponential decaying function. For increasing densities the constraint on the total surface will lead to an increasing value of  $\alpha_2$ , which becomes zero at a packing fraction  $\eta = 0.2169$  and reduced pressure  $P^* = 0.7025$ . In order for the particle-size distribution function to become bimodal, however, it should have a local minimum. This requires its derivative with respect to the surface to be zero

$$\frac{dW(s)}{ds} = W(s) \left( \frac{\alpha_1}{2\sigma} + \alpha_2 + \frac{3\alpha_3\sigma}{2} \right) = 0. \quad (9)$$

This point, which is characterized by the equation  $\alpha_2^2 = 3\alpha_1\alpha_3$ , can be numerically evaluated and leads to a critical value of the density  $\eta_C = 0.3889$  and pressure  $P^* = 3.4019$  above which bimodal behavior can be observed.

For the more accurate equation of state provided by Mansoori *et al.*<sup>5</sup>, the pressure should be replaced by

$$\frac{\pi}{6} P_{HS}^* = \frac{\xi_0}{1 - \xi_3} + \frac{3\xi_1\xi_2}{(1 - \xi_3)^2} + \frac{3\xi_2^3}{(1 - \xi_3)^3} - \frac{\xi_3\xi_2^3}{(1 - \xi_3)^3}. \quad (10)$$

This equation of state is obtained by  $P_{HS}^* = \frac{2}{3}P^* + \frac{1}{3}P_{Vir}^*$ , where  $P_{Vir}^*$  is the virial pressure. The analysis is identical to that of the PY equation of state, but leads to slightly different values.  $\alpha_2$  becomes zero at  $\eta = 0.2174$  and  $P_{HS}^* = 0.7016$ , and the critical point is found at  $\eta_C = 0.3944$  and  $P_{HS,C}^* = 3.4362$ .

The different equations of state, lead here not only to a different pressure value for given density, but also to slightly different particle-size distributions. This is in contrast with the fixed volume model, where the different equations of state for given density would only influence the value of the pressure.

### III. SIMULATIONS

For the Monte Carlo simulations we used the isothermal-isobaric ensemble or sometimes referred to as *NPT*-simulations<sup>6</sup>. This means that the number of particles  $N$ , the pressure  $P$  and the temperature  $T$  are fixed. In the simulations there are three types of trial moves. The positions of the particles are allowed to change by small amounts and we allow the simulation box to fluctuate, in order to equilibrate with respect to the applied pressure. In the case of the simulations of crystals we use a rectangular box for which the three boxlengths are allowed to change independently, while for the other simulations the shape of the simulation box remains cubic.

A third type of trial move is required in order to sample the polydispersity. To this end we select at random two particles and attempt to exchange an amount of surface between them, which is uniformly drawn from the interval  $[-\Delta S_{max}, \Delta S_{max}]$ . Here  $\Delta S_{max}$  is the maximum amount of surface we allow to be exchanged, and is adjusted such that the acceptance of this move is between 35 and 50%. Note that although the total amount of surface of the particles is fixed the volume they will occupy will change.

The equation of state, resulting from our computer simulations of the isotropic fluid performed on 1000 particles, is shown in Figs. 1 and 2. It compares nicely with the equation of state of the Percus-Yevick approximation (2). The equation of state of Mansoori *et al* (10), performs even better.

In Fig. 3 we show several particle-size distributions obtained from our simulations of the isotropic fluid. For low pressure we find an exponential decay. For the reduced pressure  $P^* = 4.0$  we observe that it is bimodal, which is in agreement with the theoretical predictions. For increasing pressure the fraction of small particles decreases. Theoretically it remains bimodal, since  $\alpha_1$  in (6) is always negative, however it becomes very small and in our simulations has disappeared at  $P^* = 20.0$ . In Fig. 4, a comparison is made between the measured and predicted distributions. As can be seen they coincide nicely up to  $P^* = 20.0$  and  $\eta = 0.568$ , and upon increasing pressure the width of the unimodal distribution decreases.

This can be partially understood by the following argument. Upon increasing pressure the system will try to adapt by forming a higher density. This can be achieved by decreasing the volume of the simulation box. One way to accomplish this would be by crystallizing. In our simulation however there is another way in which this can be achieved: decreasing the volume occupied by the particles. This is possible, because the total surface of the particles is fixed, but their total volume is free to change. If a special case of the Power Mean inequality is applied to the particle diameters we obtain

$$\sqrt[3]{\frac{1}{N} \sum \sigma_i^3} \geq \sqrt{\frac{1}{N} \sum \sigma_i^2}, \quad (11)$$

where equality only holds if all diameters are the same. Therefore the volume occupied by the particles can be lowered by forming a more uniform size-distribution.

If the pressure is increased even more the size-distribution starts to deviate again from the single peaked distribution (Fig. 3), and starts to develop second peaks. This suggest that the limit to what extend the system can equilibrate under higher pressures by becoming more uniform is reached. Although it is not observed within the duration of our simulations, one possibility is that it will try to stabilize by forming a crystalline structure with possible different sized particles.

#### IV. CRYSTAL PHASES

As mentioned in the previous section this system can equilibrate in two ways to higher pressures, by forming a more uniform size-distribution or by forming a more ordered structure. In order to explore this last possibility we tried several possibilities.

For a monodisperse system the highest density which can be obtained, would be by forming a face-centered-cubic crystal (FCC) or the hexagonal close-packed crystal (HCP). The highest packing fraction  $\eta$  which can be obtained by those crystals is  $\eta = \pi/\sqrt{18} = 0.74048$ .

In our case however we can also explore the possibilities to form crystals with two or more particle sizes. One of these possibilities is the formation of a simple cubic crystal (SC). By alternating two particle sizes, as found in a NaCl-crystal, it can be easily shown that the

highest packing fraction which this  $AB$  type crystal can reach is  $\eta = 0.79311$ . In this case the diameters in terms of the reference particle are given by 1.30656 and 0.541196. Note that for this calculation we have the additional constraint that the average particle surface is fixed.

We also considered the  $AB_2$  structure as observed for an  $\text{AlB}_2$  crystal, where hexagonal closed packed layers of larger particles are separated by hexagonal rings of smaller particles. The highest packing fraction, which can be reached by this  $AB_2$  type crystal, is  $\eta = 0.78211$  in the case that the particles have diameters 1.38828 and 0.73235.

We performed simulations starting with these three perfect crystals, using 720 particles for the FCC crystal, 1000 for the  $AB$  crystal and 864 for the  $AB_2$  crystal. For high pressures these crystals are all at least mechanically stable. The equations of state of these branches are also shown in Figs. 1 and 2. Note that due to the non-fixed occupied volume of the particles a crystal with higher packing fraction does not guarantee a higher number density. The particle-size distribution (Figs. 5, 6, 7) shows the broadening of the peaks if the pressure is lowered, and a shift of the maximum of the later two. The lowest pressure points are close to the mechanical instabilities of these crystals and give an lower bound to the coexistence pressure, if any of these crystals is thermodynamically stable.

Compression on any of these crystal branches leaves the structure intact, and the same equation of state is followed. However the compression from the isotropic fluid does not show a transition to a crystal branch. This might be due to the length of our simulation, and the slow process of forming such a crystal from an unordered system.

Although the particle-size distribution functions for the high density crystals are almost monodisperse for the FCC crystal and bidisperse for the  $AB$  and  $AB_2$  structures, it is not possible to use this in order to simplify a cell theory to only one or two particle sizes<sup>7</sup>. A comparison with simulation results of pure mono- and bidisperse systems with the “optimal” sizes, reveals a substantial difference in the equation of state (Fig. 8). Therefore polydispersity should be taken into account by incorporating the particle-size distribution function in the cell theory, which falls outside the scope of this article. As a consequence we can at this moment only conclude that these crystals are mechanically stable, but not which of them is or are thermodynamically stable.

We only considered the  $AB$  and  $AB_2$  compounds described above, because they can lead to packing fractions beyond that of a monodisperse FCC or HCP crystal. There are however more possible candidates, like the  $\text{CsCl}$  and  $\text{CaF}_2$  structures, or other compound types like  $AB_3$ ,  $AB_4$ ,  $AB_5$  and  $AB_{13}$ <sup>8</sup>. Even more complex crystals could be obtained by using three or more particles sizes. A number of these structures are probably not stable, because either the the packing fraction can not be high enough, or the smaller particles are able to escape from their lattice positions<sup>7</sup>.

## V. CONCLUSION

We have investigated a polydisperse hard sphere system in which particles can exchange surface under the constraint that the total surface of the particles is fixed. In contrast with a similar model<sup>1</sup>, the equation of state does not break down, and predictions made by the approximation of Mansoori *et al* works very well.

For low pressures the particle-size distribution is an exponential decaying function. On increasing pressure it becomes bimodal and eventually it forms a single peaked distribution by eliminating the smallest particles. If the pressure is increased even more there are signs that it might become bimodal again, e.g. by forming a crystal with two particle sizes. However, such a transition is not observed.

We performed simulations on three types of polydisperse crystals: a FCC-like crystal, an *AB*-crystal as found for NaCl, and an *AB*<sub>2</sub>-crystal as found for AlB<sub>2</sub>. These crystals are all mechanically stable, and are just the most basic types of crystals possible. The polydispersity, however, influences the equation of state such, that a simple cell theory can not predict the true coexistence or thermodynamically stable crystal for these approximately mono- and bidisperse crystals.

The formation of an “Appolonian” packing, which in principle can lead to a space-filling structure, is not likely to happen, as the constraint on the total surface prevents this. The study of this and a previous model<sup>1</sup> have shown that these simple models lead to surprising results. Although they are both somewhat artificial we hope that they will stimulate the research towards more realistic, related models.

## ACKNOWLEDGMENTS

We thank Daan Frenkel, José Cuesta and Emmanuel Trizac for a critical reading of the manuscript, as well as for their comments on and discussions about the results presented here.

## REFERENCES

- <sup>1</sup> J. Zhang, R. Blaak, E. Trizac, J. A. Cuesta, and D. Frenkel, J. Chem. Phys. **110**, 5318 (1999).
- <sup>2</sup> J. J. Salacuse and G. Stell, J. Chem. Phys. **77**, 3714 (1982).
- <sup>3</sup> R. J. Baxter, J. Chem. Phys. **52**, 4559 (1970).
- <sup>4</sup> E. Trizac, Private Communication, (1999).
- <sup>5</sup> G. A. Mansoori, N. F. Carnahan, K. E. Starling, and T. W. Leland, Jr., J. Chem. Phys. **54**, 1523 (1971).
- <sup>6</sup> D. Frenkel and B. Smit, *Understanding Molecular Simulation. From Algorithms to Applications* (Academic Press, Boston, 1996).
- <sup>7</sup> X. Cottin and P. A. Monson, J. Chem. Phys. **102**, 3354 (1995).
- <sup>8</sup> M. J. Murray and J. V. Sanders, Philos. Mag. **42**, 721 (1980).

## FIGURE CAPTIONS

1. The equation of state of the polydisperse system. The circles are the simulation results of the isotropic fluid, the squares of an FCC crystal, the diamonds of an  $AB$  crystal, and the triangles of an  $AB_2$  crystal. The theoretical predictions, Percus-Yevick (dashed) and the Mansoori *et al* (solid), are also shown.
2. The equation of state of the polydisperse system as in Fig. 1, but now the reduced pressure  $P^*$  is given as function of the reduced density  $\rho^*$ . Note that the differences are caused by the fact that the occupied volume of the particles is not fixed.
3. The particle distribution function for several reduced pressures obtained by simulations of the isotropic fluid. At reduced pressure  $P^* = 4.0$  the distribution is just bimodal. The highest pressure shown ( $P^* = 50.$ ) suggest the formation of a second peak.
4. A comparison between the particle distribution function obtained from simulation (points) and the Mansoori *et al* approximation (lines), for reduced pressures  $P^* = 4.0$ ,  $P^* = 20.$ , and  $P^* = 50..$  There is a very good agreement, except for the highest pressure where the predicted curve remains nicely single-peaked, while the simulation suggest the formation of bimodal distribution.
5. The particle distribution function for several reduced pressures on the FCC branch.  $P^* = 22.$  is the lowest pressure for which the crystal did not melt during the duration of our simulation.
6. The particle distribution function for several reduced pressures on the  $AB$ -crystal branch.  $P^* = 42.$  is the lowest pressure for which the crystal did not melt during the duration of our simulation.
7. The particle distribution function for several reduced pressures on the  $AB_2$ -crystal branch.  $P^* = 32.$  is the lowest pressure for which the crystal did not melt during the duration of our simulation.
8. A comparison of the equations of state of polydisperse and mono- or bidisperse systems. The squares correspond to a FCC crystal, the diamonds to an  $AB$  crystal, and the triangles to an  $AB_2$  crystal. The open symbols correspond to the polydisperse systems, while the filled symbols denote the results of true mono- or bidisperse systems with fixed “optimal” size ratios.

## FIGURES

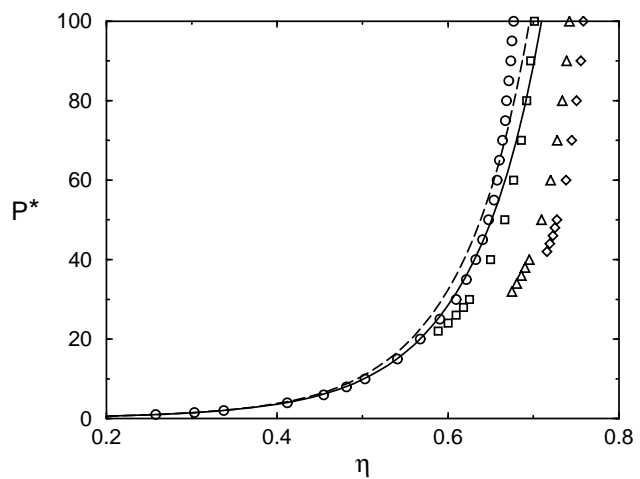


FIG. 1. Blaak, Journal of Chemical Physics

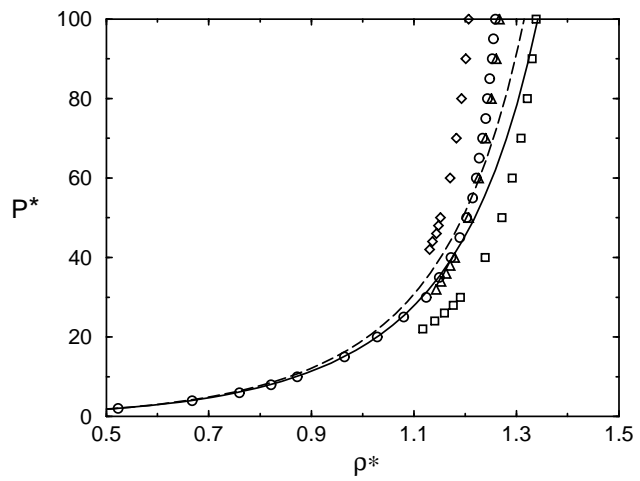


FIG. 2. Blaak, Journal of Chemical Physics

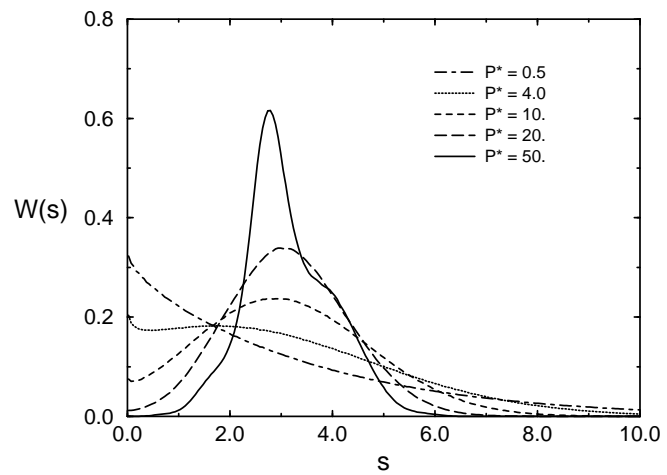


FIG. 3. Blaak, Journal of Chemical Physics

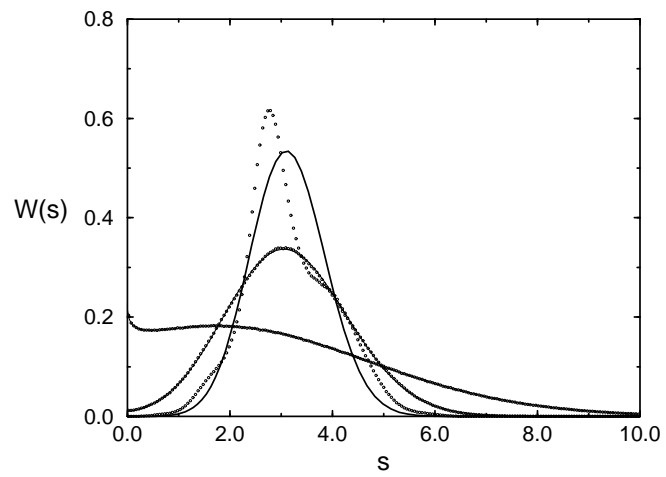


FIG. 4. Blaak, Journal of Chemical Physics

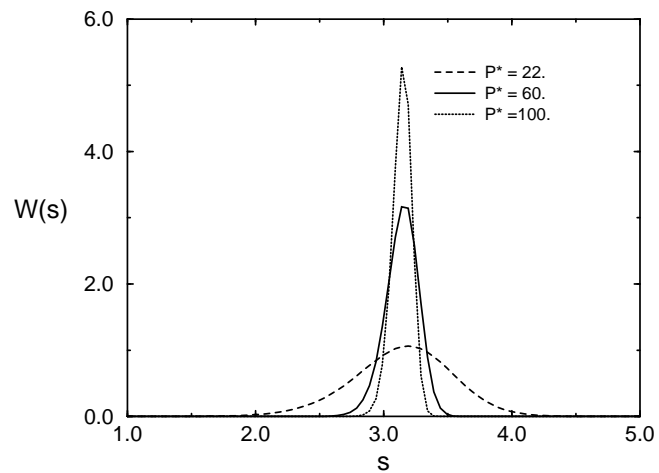


FIG. 5. Blaak, Journal of Chemical Physics

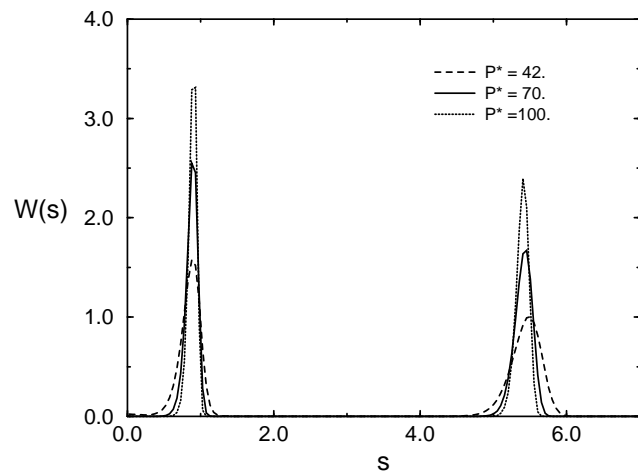


FIG. 6. Blaak, Journal of Chemical Physics

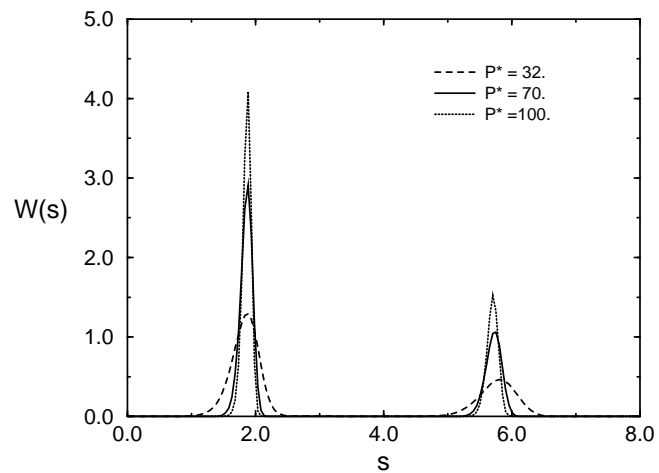


FIG. 7. Blaak, Journal of Chemical Physics

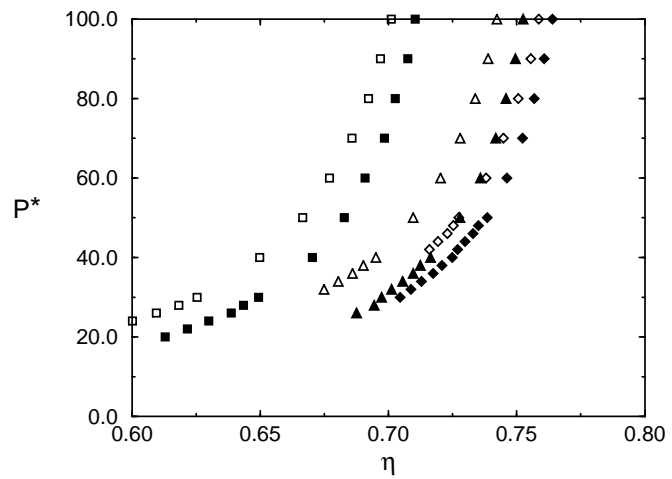


FIG. 8. Blaak, Journal of Chemical Physics